

ChemComm

Chemical Communications

Accepted Manuscript

This article can be cited before page numbers have been issued, to do this please use: J. Chen, Y. Fang, L. Sun, F. Zeng and S. Wu, *Chem. Commun.*, 2020, DOI: 10.1039/D0CC04635C.



This is an Accepted Manuscript, which has been through the Royal Society of Chemistry peer review process and has been accepted for publication.

Accepted Manuscripts are published online shortly after acceptance, before technical editing, formatting and proof reading. Using this free service, authors can make their results available to the community, in citable form, before we publish the edited article. We will replace this Accepted Manuscript with the edited and formatted Advance Article as soon as it is available.

You can find more information about Accepted Manuscripts in the [Information for Authors](#).

Please note that technical editing may introduce minor changes to the text and/or graphics, which may alter content. The journal's standard [Terms & Conditions](#) and the [Ethical guidelines](#) still apply. In no event shall the Royal Society of Chemistry be held responsible for any errors or omissions in this Accepted Manuscript or any consequences arising from the use of any information it contains.

COMMUNICATION

Activatable Probe for Detecting Alcoholic Liver Injury via Multispectral Optoacoustic Tomography and Fluorescence ImagingJunjie Chen,^a Yichang Fang,^a Lihe Sun,^a Fang Zeng*^a and Shuizhu Wu*^aReceived 00th January
20xx,

Accepted 00th January 20xx

DOI: 10.1039/x0xx00000x

A probe has been developed for imaging alcoholic liver injury through detecting the overexpressed cytochrome P450 reductase in hypoxia in hepatic region. Upon response to the enzyme, the activated probe displays turn-on fluorescence and near-infrared absorption and generates prominent optoacoustic signals.

Alcoholic liver diseases (ALD) as a result of excessive alcohol consumption are the most prevalent cause for advanced liver diseases and have become a major cause of liver-related mortality worldwide,¹ as liver is the main site for alcohol metabolism and the major target organ of alcohol-induced liver injury. Alcohol-induced liver injury is the early stage of ALD which include hepatic lesions, fatty liver, steatohepatitis, progressive fibrosis, cirrhosis and even liver failure.² Therefore, it is of great importance to detect alcohol-induced liver injury, so as to plan optimal rehabilitation program and efficacious treatment. Recent researches have shown that, in the case of alcoholic liver injury, hepatic cytochrome P450 (CYP450) reductase is overexpressed along with enhanced hypoxia extent.³⁻⁵ Therefore, the overexpression of hepatic CYP450 along with hypoxia could act as an in-situ biomarker for alcohol-induced liver injury, and methods for sensitive detection of CYP450 reductase in hypoxia in hepatic region could aid in the early diagnosis of alcohol-induced liver injury, so that effective treatment measures could be taken to prevent the liver injury from worsening into severe ALD.

Usually diagnostic methods for liver injury include blood biochemistry, histopathological examination and liver biopsy.⁶ However, these methods still have some limitations; for example, as for blood chemistry, it usually measures the levels of the enzymes that liver releases into blood, however, the enzymes also are present in other organs or tissues besides the liver, which could compromise the detection specificity and thereby could give false positive results;⁷⁻¹⁰ while histopathological examination and liver biopsy are invasive and require relatively time-consuming and complicated operation process.¹¹ Hence non-invasive fluorescent imaging method has recently been employed for detecting alcohol-induced liver injury.^{12, 13} However, strong light scattering by tissues (which scales with $\lambda^{-\alpha}$,

α reaches 4 for tissues) reduces the imaging depth and resolution,¹⁴⁻¹⁸ which would erode the performance of fluorescent imaging for liver, as liver is relatively deep seated in the body. Therefore, the imaging method with deep penetration depth and high temporal and spatial resolution for alcohol-induced liver injury would be ideal.

Optoacoustic imaging is a rapidly developing and non-invasive imaging technique with great potential for preclinical/clinical applications.^{19,20} In-vivo optoacoustic imaging could combine the advantages of optical imaging and ultrasound imaging, such as high-contrast, reduced tissues' light scattering and deep imaging depth. In particular, as a spectral optoacoustic technique, multispectral optoacoustic tomography (MSOT) operates by irradiating a sample with multiple wavelengths and then detecting ultrasound waves produced by photoabsorbers in the sample; with spectral unmixing MSOT can thus separately visualize individual photoabsorber in the target sample.^{8,20} Moreover, three-dimensional (3D) images are provided with a stack of cross-sectional images being rendered as the maximum intensity projection (MIP) images. Hence, with a suitable probe that is responsive to hepatic CYP450, MSOT imaging method would be conducive to accurately detecting alcohol-induced liver injury with 3D information in a non-invasive and spatiotemporal way.

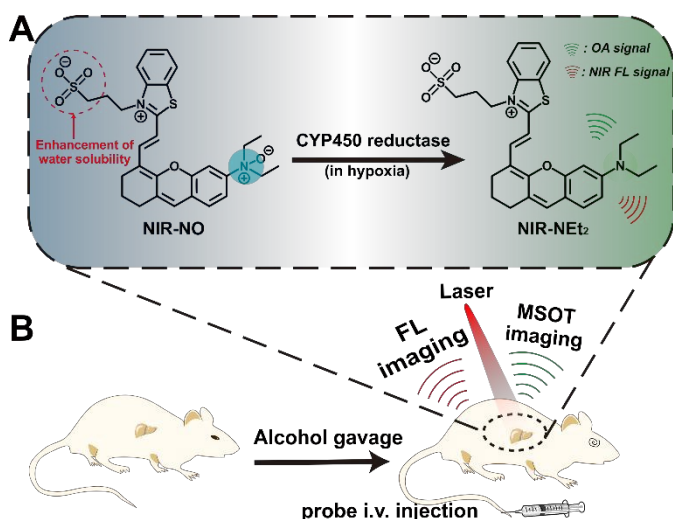
In the light of the foregoing, herein we developed an activatable and water-soluble probe (NIR-NO) for detecting alcohol-induced liver injury using the optoacoustic/fluorescent dual-mode turn-on imaging. As for the chemical structure of this probe in terms of the design rationale, a benzothiazole-xanthene chromophore serves as the reporter, while an N-oxide moiety acts as both the fluorescence quencher and the responsive unit that can undergo facile bio-reduction by CYP450 reductase with oxygen deficiency; as a result, upon response to CYP450 reductase in hypoxia, the N-oxide-containing probe NIR-NO turns into the tertiary-amine-containing chromophore (NIR-NEt₂) which elicits an enhanced fluorescence at 745 nm as well as a red shift in the absorption from 550 nm to 718 nm and correspondingly strong optoacoustic signals (as shown in Scheme 1,). Owing to the change in intramolecular electronic push-pull state with the electron-withdrawing N-oxide element turning into electron-donating group diethylamino, both the fluorescent and optoacoustic signals are turned on. The probe exhibits additional beneficial features, e.g. the introduction of sulfonate group enhances water solubility that facilitates biological applications commonly in aqueous media, and it also is conducive to the probe's reaching and accumulating in liver, furthermore the dual-mode (MSOT and fluorescent) imaging allows mutual corroboration. In vivo imaging results indicate that, the probe can quickly respond to the

^a State Key Laboratory of Luminescent Materials and Devices, Guangdong Provincial Key Laboratory of Luminescence from Molecular Aggregates, College of Materials Science and Engineering, South China University of Technology, Guangzhou 510640, China. E-mail: mcfzeng@scut.edu.cn; shzhwu@scut.edu.cn

Electronic Supplementary Information (ESI) available: [details of any supplementary information available should be included here]. See DOI: 10.1039/x0xx00000x

overexpressed CYP450 reductase in the liver region and thereby provide temporal and 3D spatial information of the disease foci for alcohol-induced liver injury.

The activatable probe was synthesized by coupling of a sulfonate-containing benzothiazole derivative with xanthene via Knoevenagel reaction, and then N-oxide was attached onto the xanthene side through oxygenation with *m*-chloroperbenzoic acid. The detailed synthetic route of the NIR-NO is given in Scheme S1. The probe NIR-NO and some intermediates were characterized by ^1H NMR and high-resolution mass spectroscopy (Fig. S1-S8).



Scheme 1 Schematic display of the probe's response to the overexpressed CYP450 reductase in hepatic region (A) and fluorescent and MSOT imaging of alcohol-induced liver injury in mouse model (B).

The spectral properties of NIR-NO were investigated with CYP450 reductase in PBS solution (pH=7.4, 10 mM, 37 °C) with oxygen deficiency. As shown in Fig. 1, in the absence of CYP450 reductase, NIR-NO is weakly emissive at 745 nm and exhibits a strong absorption at 550 nm; while incubation with CYP450 reductase gradually increases the fluorescence emission at 745 nm and the absorption red-shifts, correspondingly optoacoustic signal at around 718 nm enhances. These results demonstrate that the probe NIR-NO could be employed for both fluorescence and optoacoustic imaging via responding to CYP450. Additionally, the time-dependent spectral measurements were performed after incubating the probe with CYP450 reductase with nitrogen bubbling for varied time. As shown in Fig. S9, with the prolonged time of reaction between the probe NIR-NO and CYP450 reductase, the fluorescence intensity increases at 745 nm and the absorbance increases at 718 nm and reaches the plateau in about 10 min, indicating the fast response of the probe. In addition, the probe shows good pH stability (as shown in Fig. S10).

To test the sensing selectivity, the probe NIR-NO was treated with various potential and biologically-relevant interfering species, such as hyaluronidase, γ -glutamyl transferase, β -D-galactosidase, alkaline phosphatase, acetylcholinesterase, nitroreductase, heparinase and sulfhydryl-containing compounds like GSH and then fluorescence intensities and relative optoacoustic intensities measurements were conducted. As shown in Fig. S11-S12, NIR-NO shows high selectivity towards CYP450 reductase. Moreover, the extinction coefficient for NIR-NEt₂ (the activated probe) at 718 nm was determined to be $2.2 \times 10^4 \text{ M}^{-1} \text{ cm}^{-1}$.

As mouse liver microsomes (MLM) are rich in CYP450 reductase, we therefore evaluated the probe's response towards the enzyme *in vitro* by incubating NIR-NO with MLM with nitrogen bubbling. As shown in Fig. S13, for the probe, after treatment with MLM, the changes in fluorescence and absorption spectra are similar to those measured for the probe upon reaction with CYP450 reductase in PBS.

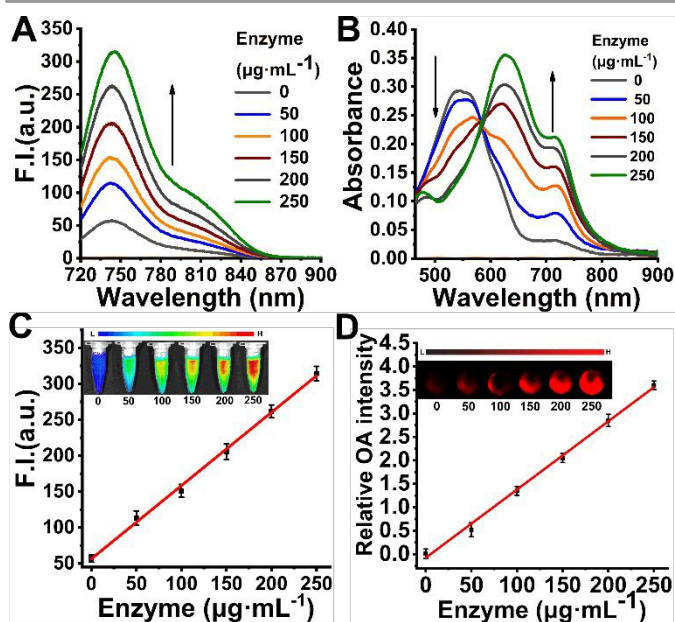


Fig. 1 (A) Fluorescence spectra (excitation: 700 nm) and (B) Absorption spectra of NIR-NO (10 μM) before and after incubation with different concentrations of CYP450 reductase with nitrogen bubbling. (C) Fluorescence intensity at 745 nm for NIR-NO (10 μM) as a function of CYP450 reductase level ($n=3$). Inset: Representative fluorescent images of the probe towards varied concentrations of CYP450 reductase. (D) Relative optoacoustic intensity $[(I-I_0)/I_0]$ for the probe upon incubation with varied concentrations of CYP450 reductase ($n=3$). Inset: Representative optoacoustic images of the NIR-NO in phantom after being incubated with varied concentrations of CYP450 reductase with nitrogen bubbling.

The research by Patterson et al. demonstrated that N-oxides could undergo two-electron reduction by CYP450 reductase in hypoxia with a heme-iron center as an active site and thus transform into tertiary amines.²¹ Based on this, the proposed mechanism for the probe's response (CYP450 mediated N-oxide reduction of the probe) is presented in Fig. S14. To confirm this mechanism, high-performance liquid chromatography (HPLC) measurement was conducted. As shown in Fig. S15, upon treatment with CYP450 reductase under hypoxia, the peak for NIR-NEt₂ (at 3.64 min) appeared while that for the NIR-NO (at 2.41 min) decreased accordingly. This demonstrates that NIR-NEt₂ is generated after incubation with CYP450 reductase under hypoxia condition.

Prior to the cell imaging, the cytotoxicities of the probe were tested by MTT assay. As shown in Fig. S16, the probe NIR-NO displays low cytotoxicity towards the HepG2 cells and L929 Cells. Notably, the cell viability remains nearly 90% even after being incubated with 50 μM of the probe. The low-toxic probe is suitable for imaging in live cells. HepG2 cells are rich in CYP450 reductase.²² Therefore, imaging of CYP450 reductase under hypoxia in HepG2 cells by the probe was conducted. From Fig. S17, we can see that the cells incubated with the probe under hypoxia for 4 h exhibit evident fluorescence

(excitation filter: 710 nm). While for the cells incubated in normoxia, weak intracellular fluorescence can be observed. For optoacoustic imaging of CYP450 reductase under hypoxia in HepG2 cells, as shown in Fig. S17, significant OA signals can be seen in the cells; while OA signals are insignificant in the cells under normoxia. To verify the OA signal and fluorescence was indeed caused by CYP450 reductase, an inhibitor of P450 reductases (diphenyl iodonium chloride (DPI), 500 μM) was used to preincubate the cells before imaging.^{23,24} As shown in Fig. S17, the DPI pretreated HepG2 cells generate very weak OA signal and weak fluorescence compared to the cells without inhibitor pretreatment. These results suggest that the probe can be activated by CYP450 reductase in hypoxia and generate optoacoustic and fluorescence signals and thus it could be used for detecting alcohol-induced liver injury via responding to hepatic CYP450 in hypoxia.

To evaluate the biosafety of the probe, the histology sections (H&E staining) of organs collected from the control and the mice intravenously injected with the probe were compared. As depicted in Fig. S18, there is no obvious histopathological difference between the sections of probe-treated mice and the control, indicating that the probe NIR-NO is biocompatible. As alcohol-induced liver injury occurs, hepatic CYP450 reductase is overexpressed with enhanced hypoxia in the liver.³ We thus investigated the probe's capability for fluorescent imaging of alcohol-induced liver injury via responding to hepatic CYP450 reductase in hypoxia. In this study, alcohol was delivered into mice by oral gavage to induce alcoholic liver injury. Then the mice were i.v. injected with the probe and fluorescent imaging was performed for varied time. The time-dependent fluorescent images for the mice pre-treated with PBS (control group), 4 $\text{g}\cdot\text{kg}^{-1}$ or 8 $\text{g}\cdot\text{kg}^{-1}$ alcohol and the rehabilitation group (treated with metadoxine) are presented in Fig. 2. It can be seen that, for the alcohol-treated mice groups, the fluorescent signals in the liver region are quite prominent after the probe injection, and reaches the maximum in about 10 min. The alcohol-treated group exhibits stronger fluorescence than the control group, and a higher dose (8 $\text{g}\cdot\text{kg}^{-1}$) of alcohol causes more prominent fluorescence, while the rehabilitation group exhibits weaker fluorescence signal. It seems that the activated probe is metabolized out of the body through the intestines. The mean fluorescent intensities obtained from the region of interest (ROI) for the four groups provide quantified fluorescence changes (Fig. 2 B). In addition, ex vivo imaging was performed for the dissected organs of the mice (Fig. 2C). As shown in Fig. 2C and Fig. S19, it is obvious that the fluorescence in liver is much stronger than other organs such as heart, spleen, lung, and kidney.

Afterwards, multispectral optoacoustic tomography was employed to image alcohol-induced liver injury in mice. Fig. 3A shows the cross-sectional images of the mice pretreated with 8 $\text{g}\cdot\text{kg}^{-1}$ alcohol at different time points after probe injection. The lower panel in this figure displays the colour images representing biodistribution of the activated probe NIR-NO₂ via spectral unmixing, while the upper panel presents the overlay of activated probe's image with the background image (at 800 nm) as an anatomical reference in which the spinal cord, thoracic aorta, and liver are labelled. At 10 min after probe injection, the signal intensity reaches the maximum. The mean signal intensities of the activated probe signal in the region of interest (ROI) over time are shown in Fig. 3B, which provides quantified evidence for the change in MSOT signals. The time-dependent MSOT signals for the other three groups (pretreated with PBS or 4 $\text{g}\cdot\text{kg}^{-1}$ alcohol and the rehabilitation group) are shown in Fig. S20 and S21. Based on the simulated cryosection image of a male mouse (Fig. 3C), it is clear that most signals from the activated probe are in the liver area. In addition, we obtained orthogonal-view 3D images for the control mice, the mice groups pretreated with

different doses of alcohol and the rehabilitation group. As shown in Fig. 3E, upon treatment with higher dose of alcohol, the signals are stronger, indicating that the CYP450 reductase in the liver is remarkably higher compared to that of the control group. While weak OA signal can be seen for the rehabilitation group.

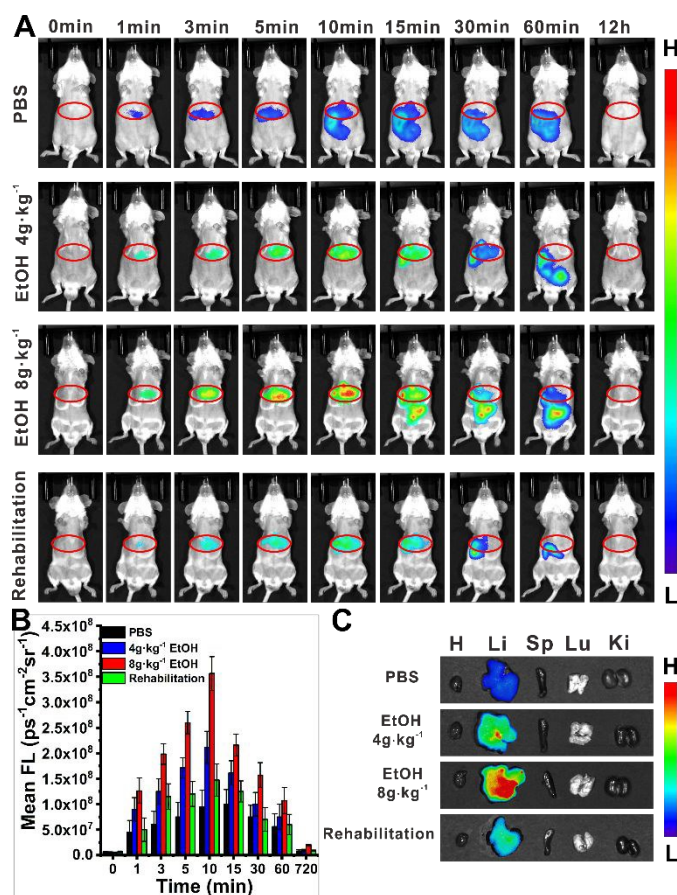


Fig. 2 Fluorescence imaging of alcohol-induced liver injury in mouse model. (A) Time course for fluorescence imaging in vivo. The mice were pretreated with PBS, 4 $\text{g}\cdot\text{kg}^{-1}$ EtOH, 8 $\text{g}\cdot\text{kg}^{-1}$ EtOH or 8 $\text{g}\cdot\text{kg}^{-1}$ EtOH + 200 $\text{mg}\cdot\text{kg}^{-1}$ metadoxine once a day for three consecutive days, followed by tail intravenous injection of 2.7 $\text{mg}\cdot\text{kg}^{-1}$ NIR-NO in PBS. (B) Mean fluorescence intensity at ROI (red-line circle) of the liver region in mice of (A). (C) Fluorescence images for major organs harvested from the mice treated with varied dose of EtOH and the rehabilitation group. (excitation filter: 710 nm, emission filter: 750 nm)

As alanine transaminase (ALT) level in blood is usually used to assess liver functions, to verify that alcohol did induce the liver injury in mice, the ALT activity in the blood of the mice was measured by Elisa kit. As shown in Fig 3D, the mice groups treated with alcohol show much higher levels of serum ALT than the control group; and the blood chemistry test results indicate that the degree of liver injury is in correlation with the dose of alcohol. Moreover, the organs of the mice treated with PBS, 4 $\text{g}\cdot\text{kg}^{-1}$, and 8 $\text{g}\cdot\text{kg}^{-1}$ of alcohol and the rehabilitation group were collected for ex vivo imaging. As shown in Fig. S22 and S23, the liver exhibits much stronger MSOT signal than other major organs. Furthermore, the liver tissue sections (H&E staining) from the mice were also examined to evaluate the liver injury, as shown in Fig. 3F, we can see that the section for the control group show no obvious pathological changes, while that for the mice

treated with alcohol exhibits necrosis with infiltration of inflammatory cells.

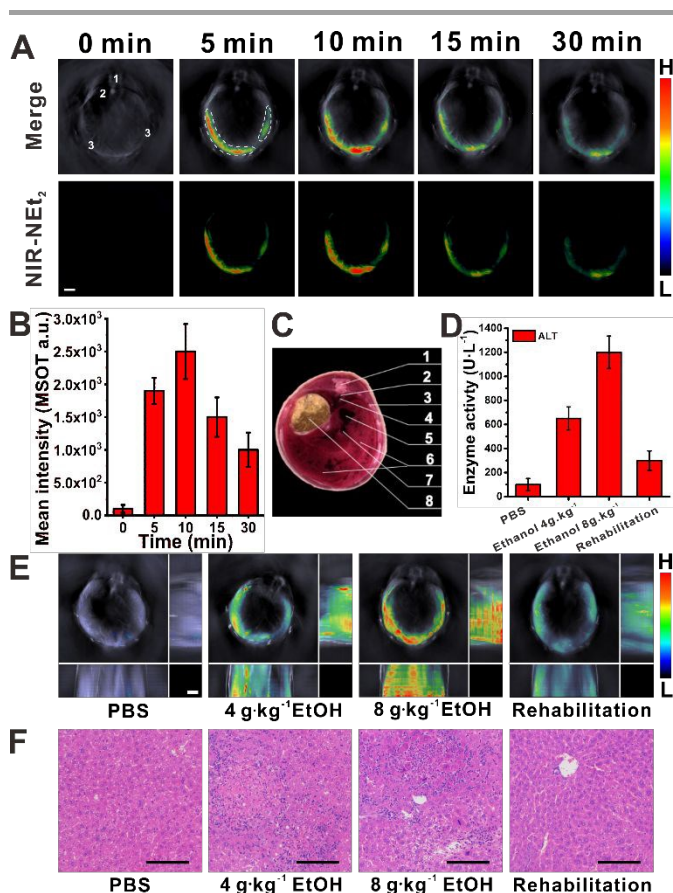


Fig. 3 (A) Representative cross-sectional MSOT images of the mouse upon injection of NIR-NO. The mouse was pre-treated with 8 g·kg⁻¹ EtOH once a day for three consecutive days. Upper panel: overlay of the activated probe NIR-NEt₂ signal with the grayscale single-wavelength (800 nm) background image. Lower panel: multispectrally resolved signal for NIR-NEt₂ (the activated probe). Organ labelling: 1. Spinal cord; 2. Aorta; 3. Liver. Scale bar: 3 mm. (B) Mean optoacoustic intensities at ROI (white dotted line) in liver area post injection of NIR-NO. (C) A cryosection image of a male mouse with the cross-section's location comparable to those shown in (A). 1. spinal cord; 2. azygos vein; 3. rib; 4. thoracic aorta; 5. vena cava; 6. liver; 7. portal vein; 8. stomach. (D) Serum levels of ALT for different mice groups. (E) Representative orthogonal-view 3D MSOT images for the mice at 10 min post i.v. injection of the probe (scale bar: 3 mm). (F) Representative H&E staining of liver sections from different mice group (scale bar: 100 μm).

In summary, a water-soluble activatable probe has been developed for detecting and imaging alcoholic liver injury in mouse model through near-infrared fluorescence and multi-spectral optoacoustic tomography imaging. Via responding in-situ to the overexpressed CYP450 reductase in hypoxia in hepatic region, the probe is activated with the N-oxide moiety being transformed into the aromatic tertiary amine group, thereby generating the NIR chromophore with enhanced fluorescence and red-shifted absorption which produce both the fluorescent and optoacoustic signals. The probe is able to image and monitor alcohol-induced liver injury and its rehabilitation in mouse model. Moreover, via MSOT

imaging the probe can locate liver injury precisely. This probe could serve as a promising tool for studying the physiological and pathological processes related to alcoholic liver diseases. And the work would offer useful insight for the design of other probes for MSOT imaging and fluorescent imaging applications in biology and medicine.

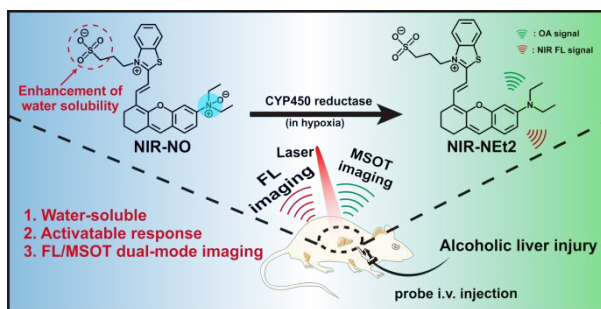
This work was supported by NSFC (21875069 and 51673066), the Natural Science Foundation of Guangdong Province (2016A030312002) and the Fund of Guangdong Provincial Key Laboratory of Luminescence from Molecular Aggregates (2019B030301003).

Conflicts of interest

There are no conflicts to declare.

Notes and references

- 1 A. Louvet and P. Mathurin, *Nat. Rev. Gastroenterol. Hepatol.*, 2015, **12**, 231-242.
- 2 J. S. Bajaj, *Nat. Rev. Gastroenterol. Hepatol.*, 2019, **16**, 235-246.
- 3 Y. Lu and A. I. Cederbaum, *Curr. Pharm. Des.*, 2018, **24**, 1502-1517.
- 4 B. Nath and G. Szabo, *Hepatology*, 2012, **55**, 622-633.
- 5 L. Gan, L. L. von Moltke, L. A. Trepanier, J. S. Harmatz, D. J. Greenblatt and M. H. Court, *Drug. Metab. Dispos.*, 2009, **37**, 90-96.
- 6 C. Moreno, S. Mueller and G. Szabo, *J. Hepatol.*, 2019, **70**, 273-283.
- 7 J. Ouyang, L. Sun, Z. Zeng, C. Zeng, F. Zeng and S. Wu, *Angew. Chem. Int. Ed. Engl.*, 2020, **59**, 10111-10121.
- 8 Y. Wu, S. Huang, J. Wang, L. Sun, F. Zeng and S. Wu, *Nat. Commun.*, 2018, **9**, 3983.
- 9 J. Li, M. A. Baird, M. A. Davis, W. Tai, L. S. Zweifel, K. M. Adams Waldorf, M. Gale, Jr., L. Rajagopal, R. H. Pierce and X. Gao, *Nat. Biomed. Eng.*, 2017, **1**, 0082.
- 10 M. M. R. Kaplan, *J. Clin. Invest.*, 1970, **49**, 508-516.
- 11 I. Mozer-Lisewska, W. Sluzewski, A. Mania, B. Walewska-Zielecka, A. Bujnowska, A. Kowala-Piaskowska and M. Figlerowicz, *Hepatol. Res.*, 2006, **34**, 9-14.
- 12 Y. Lou, C. Wang, S. Chi, S. Li, Z. Mao and Z. Liu, *Chem. Commun.*, 2019, **55**, 12912-12915.
- 13 L. Yang, Y. Chen, W. Pan, H. Wang, N. Li and B. Tang, *Anal. Chem.*, 2017, **89**, 6196-6201.
- 14 H. Zong, J. Peng, X. R. Li, M. Liu, Y. Hu, J. Li, Y. Zang, X. Li and T. D. James, *Chem. Commun.*, 2020, **56**, 515-518.
- 15 J. Xu, H. Zhang, W. Zhang, P. Li, W. Zhang, H. Wang and B. Tang, *Chem. Commun.*, 2020, **56**, 2431-2434.
- 16 G. Lv, A. Sun, M. Wang, P. Wei, R. Li and T. Yi, *Chem. Commun.*, 2020, **56**, 1625-1628.
- 17 W. L. Jiang, Y. Li, W. X. Wang, Y. T. Zhao, J. Fei and C. Y. Li, *Chem. Commun.*, 2019, **55**, 14307-14310.
- 18 Y. Qi, Y. Huang, B. Li, F. Zeng, S. Wu, *Anal. Chem.*, 2018, **90**, 1014-1020.
- 19 Y. Yan, H. Fu, J. Wang, C. Chen, Q. Wang, Y. Duan and J. Hua, *Chem. Commun.*, 2019, **55**, 10940-10943.
- 20 Y. Wu, J. Chen, L. Sun, F. Zeng, S. Wu, *Adv. Funct. Mater.*, 2019, **29**, 1807960.
- 21 L. H. Patterson, *Cancer. Metast. Rev.*, 1993, **12**, 119-134.
- 22 Y. Lu and A. I. Cederbaum, *Free. Radic. Biol. Med.*, 2008, **44**, 723-738.
- 23 H. J. Knox, T. W. Kim, Z. Zhu and J. Chan, *ACS Chem. Biol.*, 2018, **13**, 1838-1843.
- 24 H. J. Knox, J. Hedhli, T. W. Kim, K. Khalili, L. W. Dobrucki and J. Chan, *Nat. Commun.*, 2017, **8**, 1794.



An activatable probe has been developed for imaging alcoholic liver injury through detecting the overexpressed cytochrome p450 (cyp450) reductase in hypoxia in hepatic region.